Assessing the Raspberry Pi as a low-cost alternative for acquisition of near infrared hemispherical digital imagery

Kirby, Jennifer; Chapman, Lee; Chapman, Victoria

DOI:
10.1016/j.agrformet.2018.05.004

Title: Assessing the Raspberry Pi as a low-cost alternative for acquisition of near infrared hemispherical digital imagery

Authors & Affiliations:

Jennifer Kirby

University of Birmingham, College of Geography, Earth and Environmental Science, Edgbaston, Birmingham, B15 2TT, JXK067@bham.ac.uk

Professor Lee Chapman (Principle Correspondence)

University of Birmingham, College of Geography, Earth and Environmental Science, Edgbaston, Birmingham, B15 2TT, l.chapmam@bham.ac.uk

Dr Victoria Chapman

Met Office Surface Transport Team, Birmingham Centre for Railway Research and Education, Gisbert Kapp Building, University of Birmingham, Edgbaston, Birmingham, B15 2TT, victoria.chapman@metoffice.gov.uk

'Declarations of interest: none'

Abstract

Hemispherical imagery is used in many different sub-fields of climatology to calculate local radiation budgets via sky-view factor analysis. For example, in forested environments, hemispherical imagery can be used to assess the leaf canopy, (i.e. leaf area / gap fraction) as well as the radiation below the canopy structure. Nikon Coolpix cameras equipped with an FC-E8 fisheye lens have become a standard device used in hemispherical imagery analysis however as the camera is no longer manufactured, a new approach needs to be investigated, not least to take advantage of the rapid development in digital photography over the last decade. This paper conducts a comparison between a Nikon Coolpix camera and a cheaper alternative, the Raspberry Pi NoIR camera, to assess its suitability as a viable alternative for future research. The results are promising with low levels of distortion, comparable to the Nikon. Resultant sky-view factor analyses also yield promising results, but challenges remain to overcome small differences in the field of view as well as the present availability of bespoke fittings.

Comment [JK1]: Removed resolution comment

Key words: Hemispherical fisheye, Near infra-red, Raspberry Pi, Sensors

1. Introduction

Hemispherical imagery is commonly used to assist in the assessment of radiation budgets. Examples of use include below tree canopies, in urban areas or within riverine environments (*Hall et al*., 2017; *Liu et al.,* 2015; *Chapman, 2007*; *Chapman et al*; 2007; *Bréda,* 2003; *Ringold et al.,* 2003; *Watson and Johnson*, 1987). Imagery is usually obtained using a camera equipped with a fisheye lens (Figure 1a) which allows the camera to take an approx. 180˚ hemispherical image *(Liu et al., 2015; Chianucci et al., 2015).* These images are then processed to analyse the amount of visible sky shown in the image (known as the sky-view factor). This can then be used in forestry research to quantify the health of a tree and to compare differences between tree canopies *(Schwalbe et al., 2009; Leblanc et al., 2005 Jonckheere et al. 2004).*

(a) (b) (c)

Figure 1 (a) FC-E8 Fisheye lens attached to a Coolpix camera Source: Reproduced with permission from Chapman et al. (2007), copyright © 2007 IEEE, (b) First2Savv 1850 fisheye camera attached to a Samsung Galaxy S5 Neo; (c) Perspex Dome used to measure distortion.

The use of fisheye imagery for this application can be dated back to the early work of Anderson (1964), but it was the advent of digital photography which saw the approach become widely adopted. Following a number of scoping studies, which successfully compared results obtained from film cameras to the new generation of digital cameras (*Englund et al. 2000; Frazer et al. 2001; Hale and Edwards, 2002),* the new technology quickly became adopted by the scientific community. However, following the successful transition to mass digital photography, studies for the past two decades have become very reliant on the early digital cameras produced by Nikon (**Error! Reference source not found.**) such as the Coolpix 950 or 4500 *(Chianucci et al. 2016; Lang et al., 2010; Chapman, 2007; Zhang et al., 2005; Baret* *and Agroparc, 2004; Ishida, 2004).* Indeed, whilst research into hemispherical imagery has also been conducted using alternative cameras and equipment (Table 2**Error! Reference source not found.**), the Nikon Coolpix range equipped with the FC-E8 fisheye lens undoubtedly remains the most popular choice in research to date.

Seasonal Changes in Canopy Structure	
Liu et al., 2015	Used a Nikon Coolpix 4500 camera at sunset / sunrise to capture hemispherical images of tree canopies in order to investigate seasonal changes of tree canopies.
Comparing Nikon Coolpix to film cameras and Leaf canopy analysers	
Homolová et al. 2007	Used a Nikon Coolpix 8700 to compare canopy analysers to hemispherical imagery.
Garrigues, et al., 2008	Compares Nikon Coolpix 990 with LAI-2000 and AccuPAR.
Frazer et al., 2001	Compared a Nikon 950 to a film camera and highlighted the potential for blurred edges and colour distortion of a Coolpix camera but noted it can be used in calculating canopy gap measurements.
Englund et al., 2000	Compared a digital Nikon 950 and a film camera to find that low resolution images from the Nikon 950 were an adequate comparison to film cameras.
Grimmond et al., 2001	Compared a Nikon 950 Coolpix to a plant canopy analyser and found that the Nikon was an effective and easy approach to canopy analysis.

Gap function Analysis and Estimation of tree canopies	
Hu et al., 2009	Uses a Nikon 950 Coolpix camera to take hemispherical images to calculate gap size and shape within a tree canopy.
Gap function Analysis and Estimation of tree canopies	
Zhang et al., 2005	Researched the effect of exposure on calculating the leaf area index and gap function analysis using a Nikon Coolpix 4500.
Lang et al., 2010	Calculated gap function of canopies using a Nikon Coolpix 4500 and compared it to the Canon EOS 5D cameras.
Chianucci et al. 2016	Used a Nikon 4500 to compare gap functions in forested canopies.
Danson et al., 2007	A Nikon 4500 was used as a comparison to terrestrial laser scanning.
Adaption or calibration of Nikon cameras	
Chapman, 2007	Adapted a Nikon 4500 camera to make in near infra-red in order to better estimate sky-view factors and the woody bark index of tree canopies.
Baret, & Agroparc, 2004	Used a Nikon 4500 in order to determine the optical centre of an image using a fisheye lens.
Ishida, 2004	Created threshold software for colour images from a Nikon 950 camera.

Table 1 List of sample studies that use Nikon Coolpix cameras.

Studies	Camera used	Approach
Kelley and Krueger, 2005	HemiView 2.1 digital image system	Used a 20-megapixel SLR CMOS camera as part of the HemiView software (Delta Devices 2017) to record canopy structure in riparian environments
Duveiller and Defourny, 2010	Canon PowerShot A590 camera	Used a Canon PowerShot A590 camera to assess batch processing of hemispherical images
Rich, 1990	Canon T90 Minolta X700 Nikon FM2 Olympus OM4T	Comprehensive instructions on how to take hemispherical photography with a list of cameras suitable for research
Urquhart, et al., 2014	Allied Vision GE-2040C camera	Uses sky-view factors from a high dynamic range camera to calculate short term solar power forecasting
Wagner and Hagemeier, 2006	Canon AE-1 camera	Used a Canon camera to estimate leaf inclination angles on tree canopies

Table 2 Studies using alternative cameras for hemispherical photography.

The Nikon Coolpix range of cameras remains a key tool in forest climatology (**Error! Reference source not found.** and Table 2**Error! Reference source not found.**). Unfortunately, the Coolpix range is no longer readily available (*Nikon, 2016*) with digital camera technology advancing considerably in the interim making models such as the Coolpix 4500 camera appear large and bulky with a relatively poor battery life and low image resolution (3.14 megapixels). However, even today, the FC-E8 fisheye lens remains one of the least distorted on the market (*Holmer* et al., 2001) and as such, the camera series remains very popular with researchers as a tried and tested means to collect hemispherical imagery *(Chapman, 2007)*. A significant further advantage of the Coolpix range of cameras was the ability to easily convert the camera to take near infra-red (NIR) imagery. By adapting a camera in this way, it significantly enhances its functionality in the forest environment as due to the highly reflective nature of vegetation it becomes easier to distinguish this from woody elements and other features in imagery when taken in NIR; which can then be used to assess the health and density of tree canopies *(Chen et al.,* 1996; *Turner et al.,* 1999).

Overall, the Nikon Coolpix camera has reached the point where it is informally viewed as a standard device for this purpose, but with dwindling numbers now available for purchase on internet auction sites, there is a need to investigate new and more sustainable means to collect data in the long term. Whilst new digital cameras are available on the market, the approach explored in this paper is to investigate whether a low-cost alternative can be developed using readily available off-the-shelf components.

2. Methods

2.1 Adapting a Raspberry Pi

The Raspberry Pi is a range of small computers designed to minimise the cost of computing and thus make it, and computer programming more generally, accessible to a wide audience. After a prolific launch, it now has a worldwide following of developers focussed on producing generic code and peripherals for use in a range of applications. As an example, the computer can now be readily fitted with a Raspberry Pi camera and subsequently programmed to take images at set time intervals.

At the time of writing, the most popular Pi compatible camera available on the market is the Pi camera which comprises of a Sony IMX219 9-megapixel sensor. This is available either as a standard device or as a Pi NoIR camera where the infra-red blocking filter (needed by modern digital cameras due to the inherent capability to see beyond the visible spectrum: *Chapman, 2007*) has been removed (*Raspberry Pi, 2016*). As outlined in the previous section, NIR capability improves the utility of the approach for use in forested environments.

2.2 Comparison of Fisheye lenses

Unfortunately, a fisheye lens is presently not available that has been specifically designed for the Pi NoIR camera. However, due to the recent proliferation of smartphone photography, there is a wide range of fisheye lenses that are now available for smartphones which have the potential to be used. The key consideration here, as per Holmer et al, (2001), is to select a lens with minimal distortion to reduce error in later image analyses. This can be achieved by testing the equiangularity of the lens by calculating any distortions in the radial distance. As shown in Figure 2, the aim is to acquire an image where the radial distance is directly proportional to the zenith angle (*Chapman*, 2008).

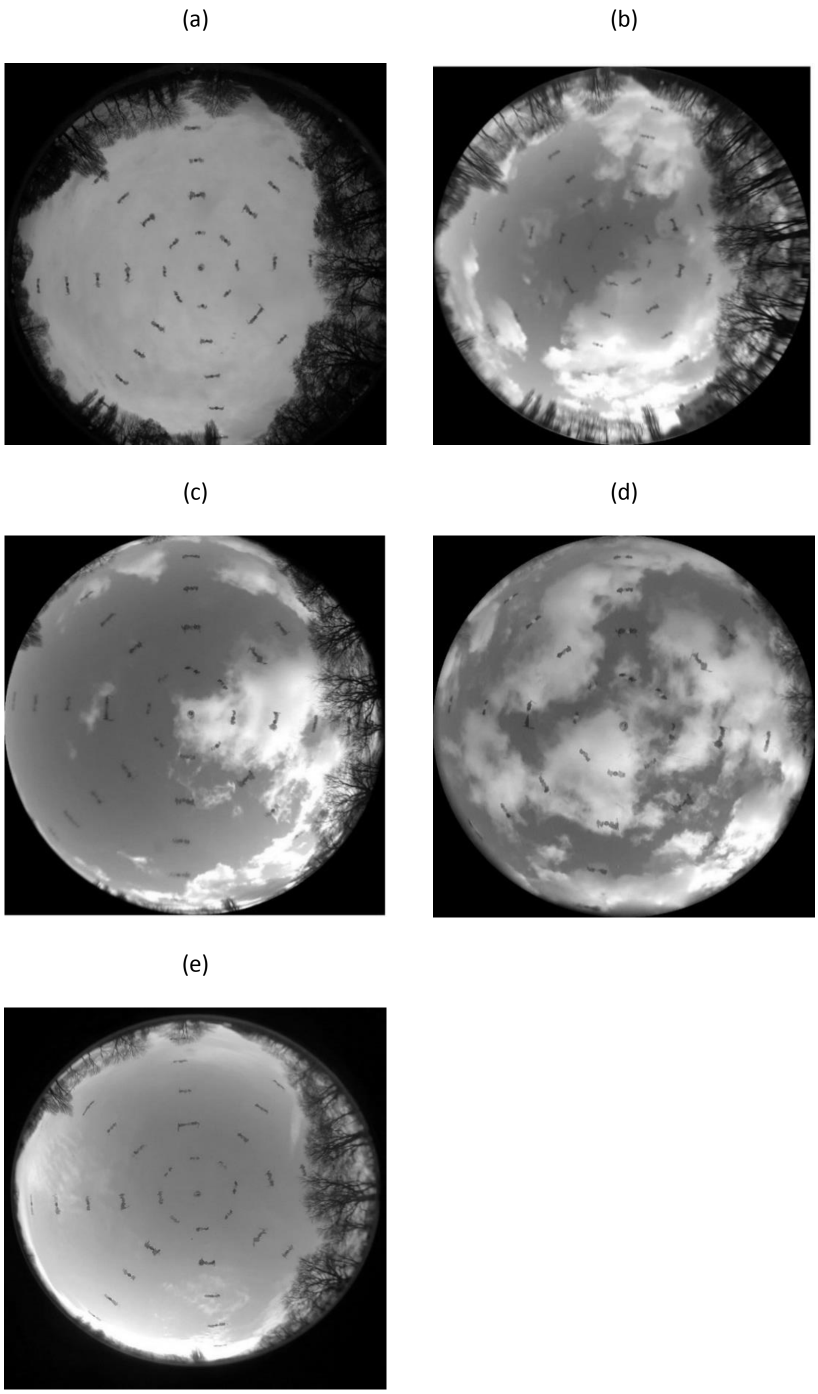

Figure 2 (a) Visual comparison of Nikon Coolpix camera, (b) smart phone camera with attached 185˚ fisheye lens, (c) smart phone camera with attached fisheye lens

198°, (d) smart phone camera with attached fisheye lens 180° and (e) smart phone camera with attached fisheye lens 235°

A range of available fisheye lenses were tested for distortions (Table 3). In this initial test, the fisheye lenses were clipped onto a Samsung Galaxy S5 Neo (Figure 1 b) and placed under a large Perspex calibration dome marked at equal points along the sides using a compass (Figure 1 c). A plumb bob was then used to position the device directly below the centre of the dome before a series of images collected (Figure 2). Measurement distortions were then calculated using Image-J software (Figure 3).

Product	Field of view	Cost (At time of writing)
Yarrashop fisheye lens	180	£7.99
First2Savv JTSJ-185-A01 fisheye lens	185	£8.99
AUKEY fisheye lens	198	£11.99
MEMTEQ universal fisheye lens	235	£10.99

Table 3 Mobile fisheye lenses specification.

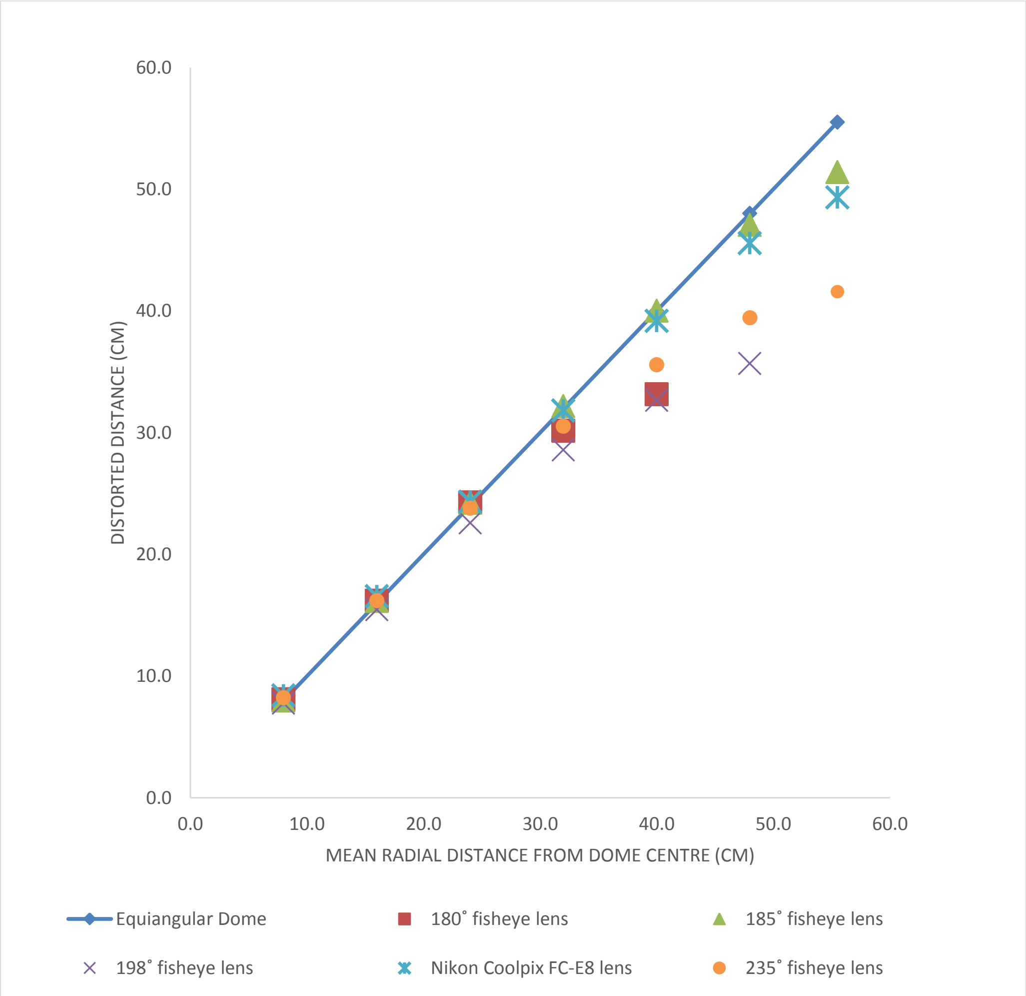

Figure 3 Comparison of radial distortion between different mobile fisheye lenses and Nikon Coolpix 4500 camera FC-E8 lens.

The results show that the 185˚ fisheye lens (Figure 2b) is most comparable with the Nikon Coolpix FC-E8 lens (Figure 2a). It has a similar field of view (FOV) and despite a slight reduction in image clarity at high radial distances, the 185˚ lens has the lowest level of distortion (Figure 3). However, comparisons between the Nikon Camera FC-E8 lens and other mobile fisheye lenses are not as favourable and all display clear distortions and/or significant reductions in FOV. For example, the 180˚ (Figure 2d) camera captures the lowest FOV of the compared fisheye lenses (Figure 3). The 198˚ fisheye lens (Figure 2c) has excellent clarity at high radial distances however has a lower FOV then reported and high levels of distortion (Figure 3). Conversely, the 234˚ fisheye lens (Figure 2e) has a high FOV however has high levels of distortion, especially at high radial distances (Figure 3). Based on these analyses, the 185˚ fisheye lens was chosen for further investigation.

2.3 Adapting a Pi Noir camera to take hemispherical images

In order to use the 185˚ fisheye lens with the Pi NoIR camera, a series of small adaptations are required. Whilst these adaptations could be achieved using 3D printing technology, this was achieved in this study using parts scavenged from the First2Savv 185º fisheye lens (Figure 4**Error! Reference source not found.**a) and tubing from a Waveshare Raspberry Pi Camera Module Kit (Figure 4b). The camera component of the Waveshare kit was removed, using a saw and drill, to leave a hollow tube. The tubing (Figure 4b) was then tied and secured to the base of the Raspberry PI NoIR camera using thin wire (Figure 4c). The camera was then attached to the Raspberry Pi board using the connector port (Figure 4d).

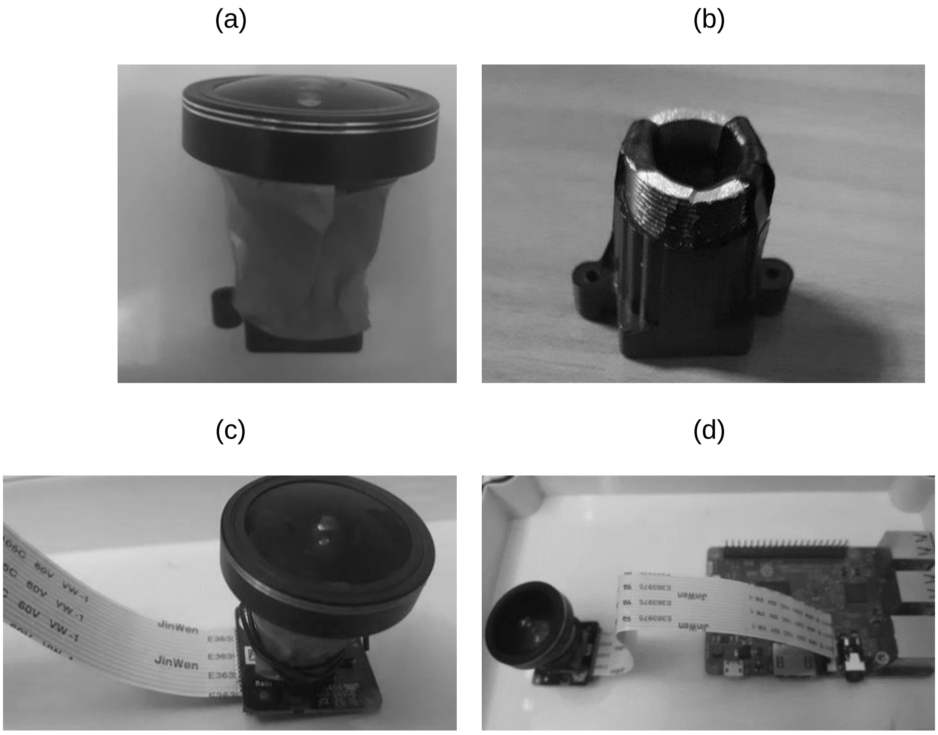

Figure 4 (a) 185° fisheye lens attached to base (b) base component of Raspberry Pi fisheye module, (c) fisheye module attached to Raspberry Pi NoIR camera (d) Camera module attached to a Raspberry Pi computer.

3. Comparison of Nikon camera and Pi NoIR Raspberry Pi camera.

3.1 General Specifications

Table 4 shows the specification comparison of both the Pi NoIR camera version 1 and 2, the Nikon Coolpix 4500 and the Nikon Coolpix 9000 camera. As has been demonstrated in the previous section, the reported FOV can vary with individual cameras (*Grimmond et al.,* 2001) and therefore this has been estimated in this study using a mechanical clinometer. The adapted Pi camera FOV (164°) is less than the

Comment [JK2]: Removed resolution argument

Nikon Coolpix FOV (176°) which is hypothesised to be a consequence of the added tubing (Figure 4b) causing some distortion and loss of image at ground level.

	Nikon 900	**Nikon 4500**	**Pi NoIR V1**	**Pi NoIR V2**
Pixel range	1.2 megapixels	3.14megapixels	5 megapixels	8 megapixels
Optical Zoom	3 x optical zoom lens	4 x optical zoom lens	N/A	N/A
Field of View	183^0 FC-E8 lens (176° using a mechanical clinometer)	183^0 FC-E8 lens (176° using a mechanical clinometer)	185^o mobile fisheye lens (164° using a mechanical clinometer)	185^o mobile fisheye lens (164° using a mechanical clinometer)
Dimensions	143 x 76.5 x 36.5mm (5.6 x 3.0 x 1.4 in.)	130 x 73 x 50mm (5.1 x 2.9 x 2.0 in.)	25 x 24 x 1mm	25 x 24 x 1mm
Cost	£100*	£200*	£25	£25

* Approximate Second-hand price

Table 4 Comparison of Coolpix cameras to Raspberry Pi cameras

3.2 Distortion Analysis

As hemispherical imagery is mostly used in the analysis of tree canopies, the loss of information at ground level (i.e. high radial distances) is less of a concern. It is at these extremities of the image where distortions are also more common and indeed one of the main attractions of the Nikon Coolpix range of cameras (*Holmer et al.*, 2001). Whilst an equiangular lens is not an essential requirement of a camera system for this application, it does ensure fewer corrections are required and minimises error in subsequent analysis. The distortions of the adapted fisheye lens are again tested by using the Perspex calibration dome (Figure **5**).

(a) (b)

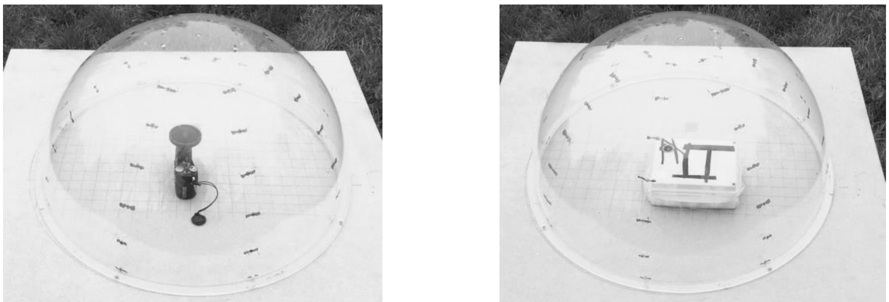

Figure 5 (a) Nikon Coolpix camera in a Perspex dome and (b) Raspberry Pi NoIR camera with fisheye attached under Perspex dome.

The FOV of the adapted Pi camera is demonstrated to be less than the Nikon camera however there is a greater level of distortion when using a Nikon Coolpix camera (

). This difference is likely due to the size of the equipment with the Nikon Coolpix camera being larger in size than the Pi camera lens (145 mm compared to 25mm). With respect to equiangularity, there is a strong correlation between radial distance distortions of the Nikon Coolpix FC-E8 lens camera and Raspberry Pi NoIR adapted fisheye camera at 99.9% confidence level (

).

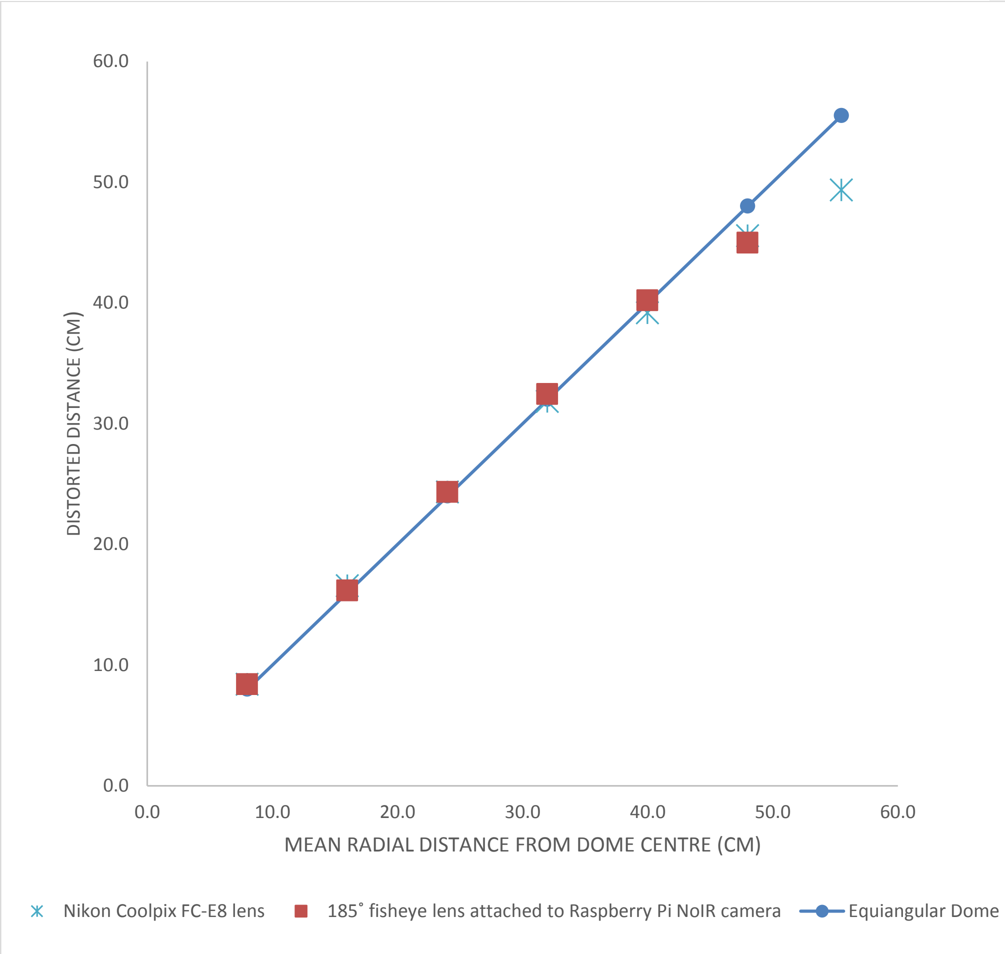

Figure 6 Radial Distortion of a Nikon Coolpix FC-E8 lens camera and a Raspberry Pi camera with attachable fisheye lens.

3.3 Sky-view factor Analysis

To further demonstrate the inter-device comparability, images were captured devices for sky-view factor analysis (

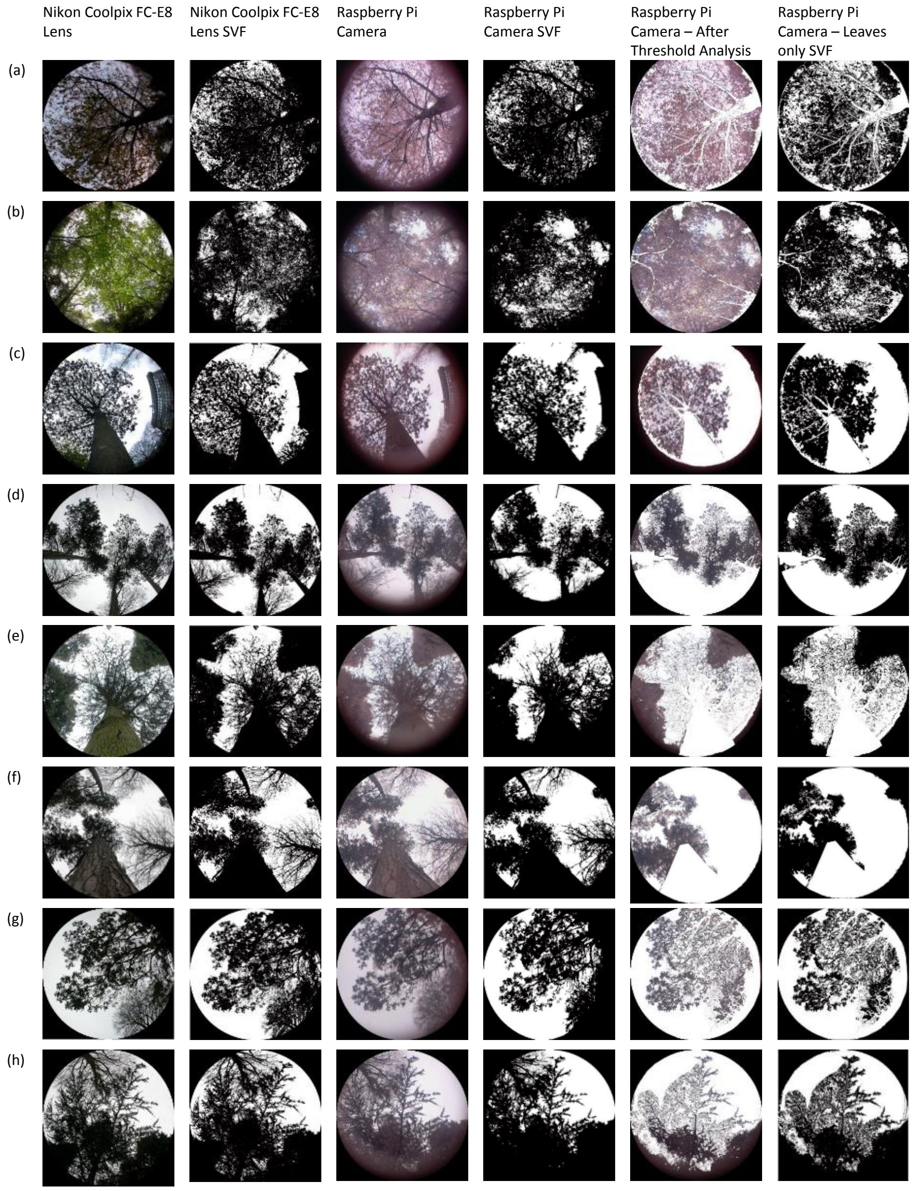

Figure 7**). The Images were then analysed using 'Sky-View Calculator' software (Göteborg Urban Climate Group, 2018) developed by Lindberg and Holmer (2010) using a process where the image was converted to binary (**

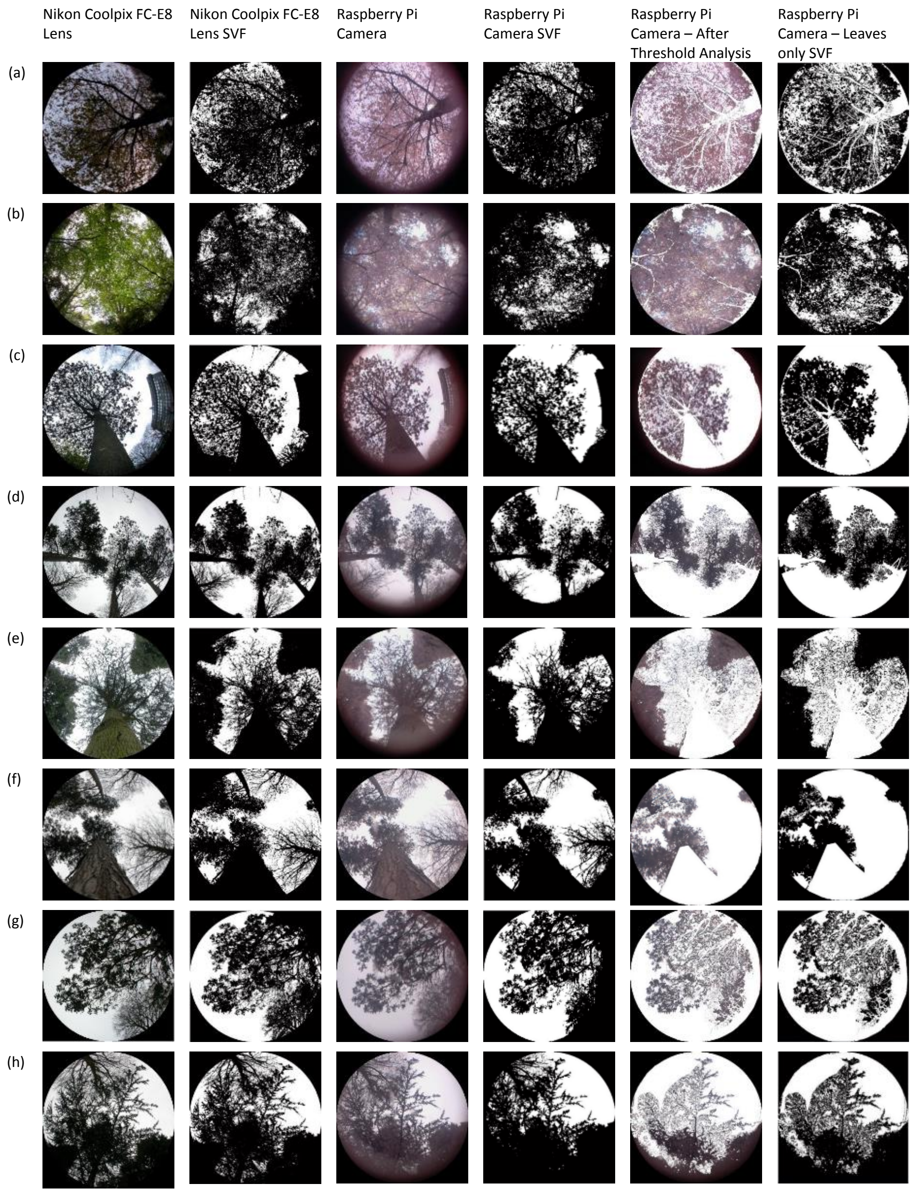

Figure **7**), divided into concentric annuli before calculating the number of white Pixels (sky) in each annulus and summed (*Holmer et al. 2001*; *Johnson and Watson, 1984;*

Steyn 1980). Analyses were performed on the original imagery as well as images cropped to have the same FOV. Table 5 shows that when the FOV is uncorrected, the Pi overestimates the sky-view factor, but when this is corrected, the output is very similar and is significant at the 99.9% level.

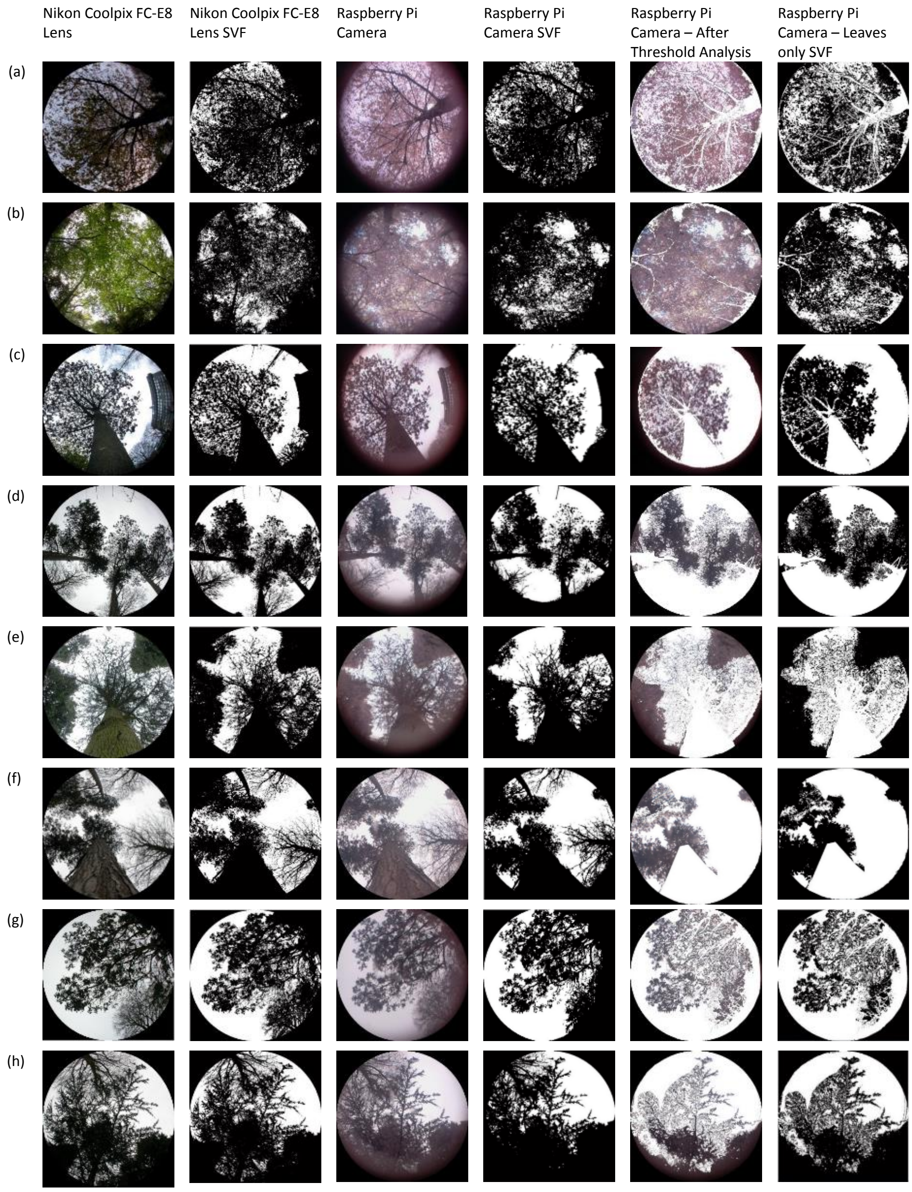

Figure 7 Visual variations in sky-view factors when comparing a Nikon Coolpix FC-E8 lens with a 185˚ Raspberry Pi NoIR camera.

Comment [JK3]: Changed an to a

Image	Sky-view factor			Leaf-view factor
	Nikon Coolpix Camera (Non-adjusted FOV)	Nikon Coolpix Camera (adjusted FOV)	Raspberry Pi Camera.	Raspberry Pi camera – contribution of leaves
(a)	0.25	0.17	0.17	0.55
(b)	0.24	0.26	0.29	0.68
(c)	0.40	0.42	0.44	0.45
(d)	0.4	0.45	0.45	0.45
(e)	0.3	0.34	0.35	0.26
(f)	0.4	0.45	0.47	0.33
(g)	0.37	0.40	0.44	0.42
(h)	0.48	0.33	0.34	0.53

Table 5 Sky view factors of Nikon Coolpix camera adjusted FOV, Raspberry Pi NoIR camera, Nikon Coolpix unadjusted FOV and Raspberry Pi leaves only images.

3.4 Near Infrared Capabilities

In addition to hardware availability, the advantages of using a Raspberry Pi NoIR camera over a Nikon 4500 camera is the in-built near infra-red (NIR) technology.

Comment [JK4]: Removed resolution argument

Although it is also possible to convert the Nikon Coolpix camera to take NIR images (*Chapman*, 2007), this involves substantial effort which risks damaging the camera.

The capability of the Pi NoIR was confirmed in this study. A simple threshold analysis proved sufficient to remove all other aspects of the image except for vegetation (

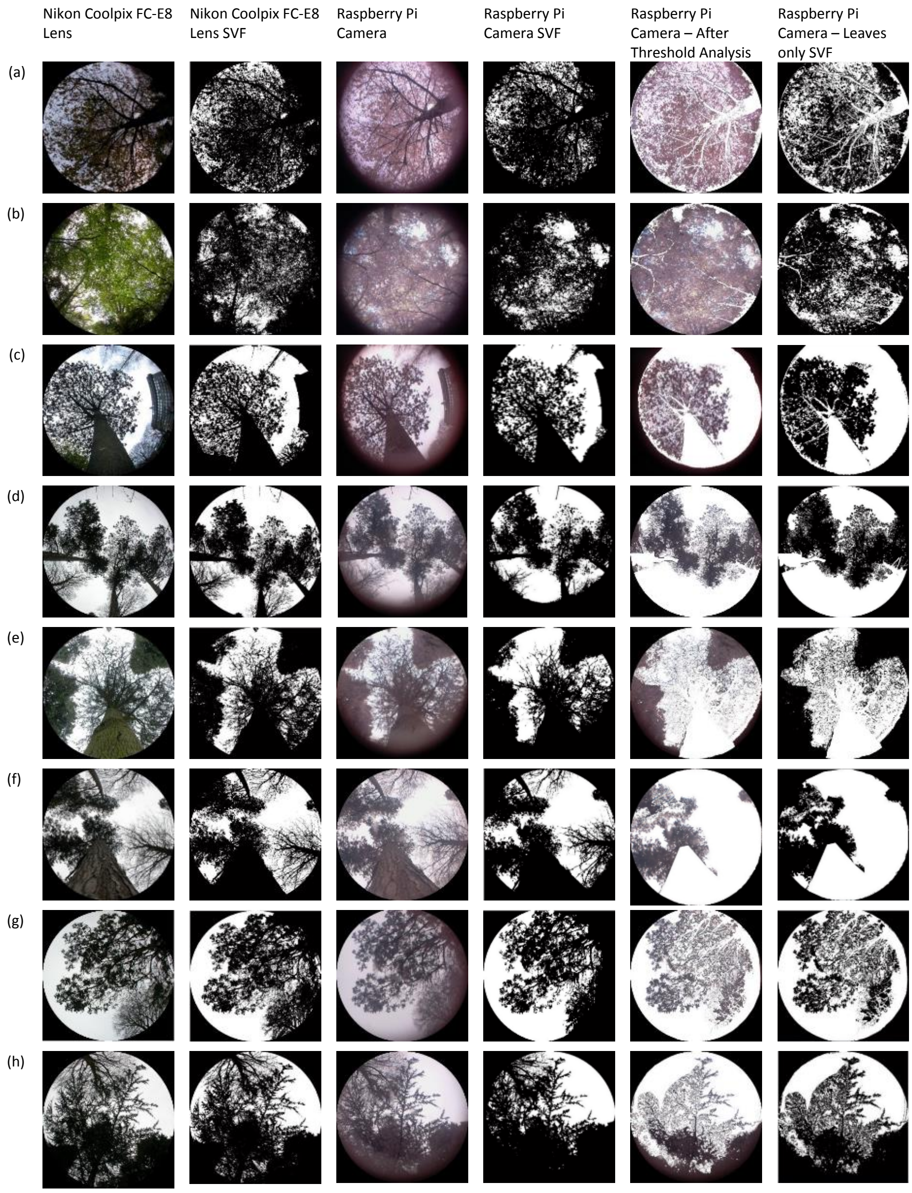

Figure **7**Table 5). The differences in sky-view factor can then be calculated; from this a leaf-view calculation were made and presented in Table 5, indicating an approximation of leaf cover in the image and further highlights the utility of the camera in forestry applications.

4. Conclusions

The Nikon Coolpix camera range has provided a reliable 'standard' solution for obtaining hemispherical fisheye imagery for many years. However, whilst still fit for purpose, an alternative is needed to ensure a sustainable means of data collection moving forward. This paper has shown that comparable results can be provided with a low-cost image collection system using readily available components.

Comment [JK5]: Removed resolution comment

The Pi NoIR camera provides an off-the-shelf NIR solution, making it perfect for use in forested environments and thus removing the need for further adaptation (i.e. removal of blocking filters and addition of cold mirrors: *Chapman, 2007*). However, fisheye lenses are not yet readily available and hence there is presently a need to carry out alternative adaptations such as those outlined in this paper, or the use of simple 3D printing technology. However, the most positive result from this study is the direct comparability of the imagery (and subsequent results from sky-view factor analyses) obtained from the two techniques. Both systems have similarly low levels of distortion, but there are minor differences in relation to the FOV. Further research is needed to adapt the Raspberry Pi to make the sensor usable in the field; this includes waterproofing the technology and testing the equipment at various temperature ranges. A limitation of this study is that the technology was not tested for interference from electronic or radio waves.

Further advantages of the Raspberry Pi approach are the computing capability of the device, which means it has internal logging capabilities and (once waterproofed) could be left in the field in time lapse mode for long periods at a time, even relaying imagery over the internet in real-time if communications are available. Overall, moving forward there are many advantages to using the Raspberry Pi, however the key conclusion is that a fit for purpose and dynamic solution for the collection of hemispherical imagery can be readily produced at a low cost.

Acknowledgements

Funding for this research was provided by the Rail Safety and Standards Board (RSSB) and the Engineering and Physical Sciences Research Council (EPSRC).

References

1. **Anderson, M.C.** 1964: Studies of Woodland light climate. *Journal of Ecology* 52, 27-41
2. **Baret, F**. and **Agroparc, S.** 2004: A simple method to calibrate hemispherical photographs. INRA-CSE, France (http://147.100.66.194/can_eye/hemis_calib3. pdf).
3. **Bréda, N. J.** 2003: Ground-based measurements of leaf area index: a review of methods, instruments and current controversies. *Journal of experimental botany*, 54(392), 2403-2417
4. **Chapman, L.** 2008: An introduction to upside-down remote sensing, *Progress in Physical Geography* 32 (5), 529-542
5. **Chapman, L.** 2007: Potential applications of near infra-red hemispherical imagery in forest environments. *Journal of Agricultural and Forest Meteorology*, 143(1), 151-156.

6. **Chapman, L., Thornes, J. E., Muller, J. P.,** and **McMuldroch, S.** 2007: Potential applications of thermal fisheye imagery in urban environments*. IEEE Geoscience and Remote Sensing Letters*, 4(1), 56-59.
7. **Chen, J. M.** 1996: Optically-based methods for measuring seasonal variation of leaf area index in boreal conifer stands*. Journal* of *Agricultural and Forest Meteorology,* 80(2-4), 135-163.
8. **Duveiller, G**., and **Defourny, P**. 2010: Batch processing of hemispherical photography using object-based image analysis to derive canopy biophysical variables. *Proceedings of GEOBIA*, 1682-1777.
9. **Chianucci, F**, **Leonardo D, Donatella G, Daniele B, Vanni N, Cinzia L, Andrea R and Piermaria C** 2016: "Estimation of canopy attributes in beech forests using true colour digital images from a small fixed-wing UAV." International journal of applied earth observation and geoinformation 47. 60-68.
10. **Chianucci, F., Macfarlane, C., Pisek, J., Cutini, A**., and **Casa, R**. 2015: Estimation of foliage clumPing from the LAI-2000 Plant Canopy Analyzer: effect of view caps. *Trees*, 29(2), 355-366.
11. **Danson, F. M., Hetherington, D., Morsdorf, F., Koetz, B.,** and **Allgower, B**. 2007: Forest canopy gap fraction from terrestrial laser scanning. *IEEE Geoscience and remote sensing letters*, 4(1), 157-160.
12. **Englund, S. R., O'brien, J. J.,** and **Clark, D. B**. 2000: Evaluation of digital and film hemispherical photography and spherical densiometry for measuring forest light environments. *Canadian Journal of Forest Research*, 30(12), 1999-2005.

13. **Delta** 2017: HemiView Forest Canopy Image Analysis System, https://www.delta-t.co.uk/product/hemiview/ accessed 30/01/2018

14. **Frazer, G. W., Fournier, R. A., Trofymow, J. A.,** and **Hall, R. J.** 2001: A comparison of digital and film fisheye photography for analysis of forest canopy structure and gap light transmission. *Journal of Agricultural and forest meteorology*, 109(4), 249-263.

15. **Garrigues, S., Shabanov, N. V., Swanson, K., Morisette, J. T., Baret, F.**, and **Myneni, R. B.** 2008: Intercomparison and sensitivity analysis of Leaf Area Index retrievals from LAI-2000, AccuPAR, and digital hemispherical photography over croplands. *Journal of Agricultural and Forest meteorology*, 148(8), 1193-1209.

16. **Grimmond, C. S. B., Potter, S. K., Zutter, H. N**., and **Souch, C.** 2001: RaPid methods to estimate sky-view factors applied to urban areas. *International Journal of Climatology,* 21(7), 903-913

17. **Göteborg Urban Climate Group**, 2018: Sky-view Calculator, University of Göthenburg, https://gvc.gu.se/english/research/climate/urban-climate/software/download. Accessed 30/01/2018

18. **Hale, S. E**., and **Edwards, C.** 2002: Comparison of film and digital hemispherical photography across a wide range of canopy densities. *Journal of Agricultural and Forest Meteorology,* 112(1), 51-56.

19. **Hall, R. J., Fournier, R. A.,** and **Rich, P.** 2017: Introduction. In Hemispherical Photography in Forest Science: *Theory, Methods, Applications* (pp. 1-13). Springer Netherlands.

20. **Holmer, B., Postgård, U**. and **Eriksson, M**., 2001: Sky view factors in forest canopies calculated with IDRISI. *Theoretical and Applied Climatology*, 68(1), pp.33-40.
21. **Homolová, L., Malenovský, Z., Hanuš, J., Tomášková, I., Dvořáková, M**., and **Pokorný, R**. 2007: Comparaison of different ground techniques to map leaf area index of Norway spruce forest canopy. *In Proceedings of the International Society for Photogrammetry and Remote Sensing* (ISPRS)
22. **Hu, L., Gong, Z., Li, J.,** and **Zhu, J**. 2009: Estimation of canopy gap size and gap shape using a hemispherical photograph. *Trees*, 23(5), 1101-1108.
23. **Ishida, M.** 2004: Automatic thresholding for digital hemispherical photography. *Canadian Journal of Forest Research*, 34(11), 2208-2216.
24. **Johnson, G. T.,** and **Watson, I. D.** 1984: The determination of view-factors in urban canyons. *Journal of Climate and Applied Meteorology*, 23(2), 329-335.
25. **Jonckheere, I., Fleck, S., Nackaerts, K., Muys, B., CopPin, P., Weiss, M**., and **Baret, F**. 2004: Review of methods for in situ leaf area index determination: Part I. Theories, sensors and hemispherical photography. *Journal of Agricultural and Forest meteorology*, 121(1), 19-35.
26. **Kelley, C.E**. and **Krueger, W.C.,** 2005: Canopy cover and shade determinations in riparian zones. *Journal of the American Water Resources Association*, 41(1), pp.37-046.
27. **Lang, M., Kuusk, A., Mõttus, M., Rautiainen, M.,** and **Nilson, T**. 2010: Canopy gap fraction estimation from digital hemispherical images using sky radiance models and a linear conversion method. *Journal of Agricultural and Forest Meteorology,* 150(1), 20-29.

28. **Leblanc, S. G., Chen, J. M., Fernandes, R., Deering, D. W**., and **Conley, A.** 2005: Methodology comparison for canopy structure parameters extraction from digital hemispherical photography in boreal forests. *Journal of Agricultural and Forest Meteorology*, 129(3),187-207.
29. **Lindberg, F.,** and **Holmer, B.** 2010: Sky View Factor Calculator, Göteborg Urban Climate Group, Department of Earth Sciences, University of Gothenburg
30. **Liu, Z., Wang, C., Chen, J. M., Wang, X**., and **Jin, G.** 2015: Empirical models for tracing seasonal changes in leaf area index in deciduous broadleaf forests by digital hemispherical photography. *Journal of Forest Ecology and Management,* 351, 67-77.
31. **Nikon**, CoolPix 4500 product archive, 2017: http://imaging.nikon.com/lineup/CoolPix/others/4500/ accessed 30/01/2018
32. **Raspberry Pi** 2016: https://www.RaspberryPi.org/products/Pi-noir-camera/, Accessed 2017
33. **Rich, P. M.** 1990: Characterizing plant canopies with hemispherical photographs. *Remote sensing reviews,* 5(1), 13-29.
34. **Ringold, P. L., Sickle, J., Rasar, K**., and **Schacher, J**. 2003: Use of hemispheric imagery for estimating stream solar exposure. *Journal of the American Water Resources Association*, 39(6), 1373-1384.
35. **Schwalbe, E., Maas, H. G., Kenter, M.,** and ***Wagner, S.*** 2009: Hemispheric image modeling and analysis techniques for solar radiation determination in forest ecosystems. *Journal of Photogrammetric Engineering and Remote Sensing,* 75(4), 375-384.

36. **Steyn, D.G.,** 1980: The calculation of view factors from fisheye-lens photographs: Research note.

37. **Turner, D. P., Cohen, W. B., Kennedy, R. E., Fassnacht, K. S.,** and **Briggs, J. M.** 1999: Relationships between leaf area index and Landsat TM spectral vegetation indices across three temperate zone sites. *Remote sensing of environment*, 70(1), 52-68.

38. **Urquhart, B., Kurtz, B., Dahlin, E., Ghonima, M., Shields, J. E.,** and **Kleissl,** J. 2014: Development of a sky imaging system for short-term solar power forecasting. *Atmospheric Measurement Techniques Discussions*, 7, 4859-4907.

39. **Wagner, S.,** and **Hagemeier, M.** 2006: Method of segmentation affects leaf inclination angle estimation in hemispherical photography. *Journal of Agricultural and Forest Meteorology*, 139(1), 12-24.

40. **Watson, I. D.,** and **Johnson, G. T.** 1987: Graphical estimation of sky view-factors in urban environments. *Journal of Climatology*, 7(2), 193-197.

41. **Zhang, Y., Chen, J.M**. and **Miller, J.R**., 2005: Determining digital hemispherical photograph exposure for leaf area index estimation. *Agricultural and Forest Meteorology*, *133*(1-4), pp.166-181.